Eur. Phys. J. Special Topics **223**, 649–663 (2014)

DOI: 10.1140/epjst/e2014-02131-1

THE EUROPEAN PHYSICAL JOURNAL SPECIAL TOPICS

Review

Order and disorder in coupled metronome systems

Sz. Boda[1], L. Davidova[1], and Z. Néda[1,2]

[1] Babeş-Bolyai University, Department of Physics, Str. Kogălniceanu 1, nr. 1, 400084 Cluj-Napoca, Romania
[2] Edutus College, Department of Mechatronics, Optics, Mechanical Engineering and Informatics, Bertalan Lajos Street 4-6, Budapest, Hungary

Received 3 March 2014 / Received in final form 18 March 2014
Published online 28 April 2014

Abstract. Metronomes placed on a smoothly rotating disk are used for exemplifying order-disorder type phase-transitions. The ordered phase corresponds to spontaneously synchronized beats, while the disordered state is when the metronomes swing in unsynchronized manner. Using a given metronome ensemble, we propose several methods for switching between ordered and disordered states. The system is studied by controlled experiments and a realistic model. The model reproduces the experimental results, and allows to study large ensembles with good statistics. Finite-size effects and the increased fluctuation in the vicinity of the phase-transition point are also successfully reproduced.

1 Introduction

Synchronization of interacting clocks is a fascinating and pedagogical example for order-disorder type phase-transitions. The phenomenon is interesting in many other aspects as well, offering an affordable pedagogical tool for discussing and exemplifying interesting topics in statistical physics. It can be used for illustrating the Kuramoto type order-disorder phase transition [1], to study finite size effects in the vicinity of the phase-transition point, for discussing issues related to dynamical systems or even the second law of thermodynamics.

Huygens' [2] observation on the strange sympathy of pendulum clocks coupled through a common suspension beam is seemingly the first recorded document on this emerging collective behavior. Many recent studies have aimed at reconsidering in various forms Huygens' two pendulum-clock experiment as well as realistically modeling the system. After more than three centuries, Huygens' experiment was reconsidered by Bennet et al. [3]. They investigated the same two pendulum-clock system as Huygens did, with a few modifications: changed the supporting mechanism, worked with newer clocks and increased precision. Bennet et al. came to many interesting conclusions, observing that several types of collective dynamics are possible, depending on the system's parameters. Synchronization occurs, if the difference between the natural frequencies of the clocks is small enough, and it occurs always as anti-phase synchronization. For strong coupling, a "beat death" phenomenon occurs when one

pendulum keeps to oscillate and the other stops. For weak coupling a quasi periodic oscillation can be observed, but synchronization does not occur. Bennet et al. also found, that anti-phase synchronization occurs just when the difference between the clocks natural frequencies is below $\delta\omega < 0.0009\,\mathrm{Hz}$ which means that the difference in the pendulums rods' length must be $\delta l < 0.02\,\mathrm{mm}$, a precision which was quite hard to achieve in Huygens time, according to Bennet et al. [3]. Hence, they attribute Huygens' observation to "talent and luck".

Kumon and his group [4] studied a similar system consisting of two pendulums, one of them having an excitation mechanism, and the two pendulums being coupled by a weak spring. Fradkov and Andrievsky [5] developed a model for such a system, and obtained from numerical solutions that both in- and anti-phase synchronizations are possible, depending on the system parameters and initial conditions.

The most complete analysis for Huygens' clocks experiment was made by Kapitaniak et al. who summarized their findings in a review article [6]. By revisiting the same experiment [7,8] they confirmed that usually the anti-phase synchronization emerges, while in-phase synchronization is possible only in some rare cases. They developed also a more realistic model which reproduced well the experimental results [7,8].

Due to the fact that mechanical pendulum clocks are quite expensive and hard to be found, nowadays instead of pendulum clocks such experiments are performed by using the more affordable metronomes. Panteleone [9] proposed a simple mechanical setup in such sense by using two metronomes placed on a light and easily movable platform. In his experiment synchronization could be observed acoustically (recording the metronomes beats) or visually by following the metronomes' pendulums. Pantaleone found that for metronomes that had small differences in their natural frequencies, synchronization emerged in a time interval of the order of tens of seconds independently of the initial conditions. It is important to remark that contrary to the previous studies on pendulum clock systems, consistently Pantaleone found just in-phase synchronization for the metronomes. In his work, he mentions also a few exceptions, but these exceptions were seeming unrepeatable with his simple experimental setup. He also found that for larger frequency differences between the oscillators natural frequencies synchronization does not occur. This result is consistent with the findings of the Kuramoto model, since the model indicates that the critical coupling strength above which synchronization emerges is linearly dependent on the standard deviation of the oscillators natural frequencies.

Pantaleone derived also approximate equations of motions for the time-evolution of the metronome ensemble. In his model the challenge was, to properly model the damping and escapement mechanism of the metronomes. Pantaleone did this by using van der Pol oscillators [10]. In the discussion section of his paper he suggested that extending the model to a multi-metronome system would provide additional opportunities in observing many interesting behavior. Ulrichs et al. [11], successfully realized this extension and studied numerically the behavior of up to 100, globally coupled units. They reported that the Kuramoto-type order-disorder phase-transition is observable in their system as well and confirmed the absence of anti-phase synchronization in the model.

Very recently our group reconsidered the metronome synchronization problem experimentally and through computer simulations of a realistic model [12]. Metronomes were placed on the perimeter of a smoothly rotating disk, and photoelectric sensors were mounted within the metronomes in order to monitor their phases. This experimental setup revealed how synchronization emerges, and also proved that such systems exhibit order-disorder type phase transitions. The rotating platform induced a global coupling between the metronomes, and the strength of the interaction between the metronomes was varied by rotating the metronomes swinging plane relative

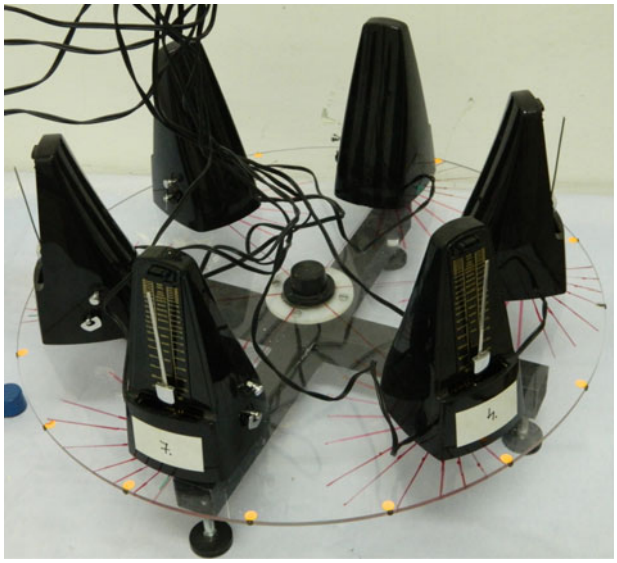

Fig. 1. Experimental setup: metronomes are placed on the perimeter of a disk that can rotate around a vertical axes.

to the radial direction on the disk. As a function of the rotating angle a transition from spontaneously synchronized to unsynchronized state was observable [13]. By varying the metronomes number on the disk finite-size effects in the vicinity of a phase-transition point were studied. In agreement with all previous studies considered in metronome systems, only in-phase synchronization was found.

In the present study we continue to investigate the coupled metronome system suggesting other feasible methods for realizing the order-disorder type phase transition. For the sake of completeness we summarize our earlier experimental results and present new results in context of these. Experimental results will be compared with numerical results obtained on a realistic model.

2 Experiments

The experimental setup is shown in Fig. 1. Metronomes are placed on the perimeter of a smoothly rotating disk. The rhythm of the metronomes are given by a physical pendulum, which consists of a rod with two weights on it (Fig. 2): a fixed one at the lower end of the rod denoted by W_1 and a movable one W_2, attached to the upper part of the rod ($W_1 > W_2$). This physical pendulum oscillates around a horizontal suspension axes. By sliding the W_2 weight on the rod, the oscillation frequency can be tuned. There are several marked places on the rod where the W_2 weight has a stable position, yielding standard ticking frequencies for the metronome. These frequencies are marked on the metronome in the units: Beats Per Minute (BPM). The exciting mechanism of the metronomes is built in the box and has the aim to compensate the energy of the pendulum lost by frictions. This mechanism delivers pulses to the physical pendulum at a given phase of the oscillation period [7].

For the experiments we selected seven *Thomann 330* metronomes, so that their standard ticking frequencies be as similar as possible. Since there are no two identical units, we still had a non-zero standard deviation of their natural frequencies. In some of the experiments we used all metronomes, and in some experiments we

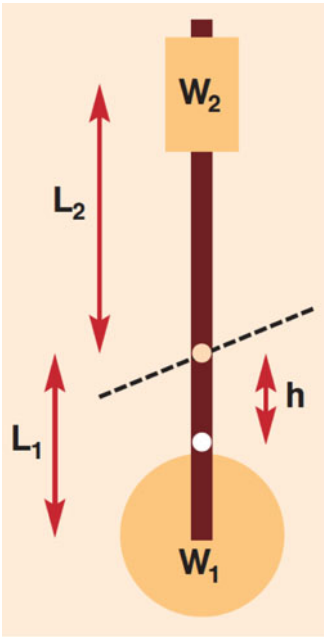

Fig. 2. Schematic view of the metronomes' bob. The dotted line denotes the horizontal suspension axes, and the white dot illustrates the center of mass.

worked with only six or even four of them (reducing further the standard deviation of their frequencies). Photo-cell detectors were mounted inside them, allowing to separately detect the phase of each pendulum. The photo-cells were connected with a circuit board, allowing data collection through the USB port of a computer. From the collected data the classical, r, Kuramoto [1] order parameter was computed:

$$r\exp(i\Psi) = \frac{1}{N}\sum_j \exp(i\beta_j). \tag{1}$$

Here Ψ is an average phase of the whole ensemble, β_j is the phase of the j-th metronome, N is the number of metronomes, and i is the imaginary unit. This order parameter is justified and captures the level of synchrony in the system since we never observed states where two synchronized clusters of metronomes are in anti-phase synchrony with each other. Characterizing such states would require a more complex order parameter. More details about the experimental method are given in our previous work [12].

Initially we monitored separately each metronome, and recorded their natural frequency for all the standardly marked rhythms. From these values the standard deviation of the metronomes' natural frequencies could be determined.

We have to emphasize from the beginning, that independently of the chosen initial condition, only in-phase synchronization of the metronomes was observed.

For illustrating the order-disorder type phase transition in this system three different kind of experiments were performed. These experiments are conceived in such manner that in a direct or indirect manner the coupling strength κ between the metronomes are controlled. By doing this we plan to show the Kuramoto-type phase transition [1], where one expects no synchronization ($r = 0$ for an infinite system or $r \propto 1/\sqrt{N}$) for $\kappa < \kappa_c$ and some level of synchrony ($r > 0$) for $\kappa > \kappa_c$.

Table 1. Standard deviation of the experimentally used seven metronomes for different nominal frequencies.

$\omega(BPM)$	160	168	176	184	192	208
$\sigma\ (BPM \cdot 10^{-7})$	8.4	7.9	7.8	9.8	8.5	8.7

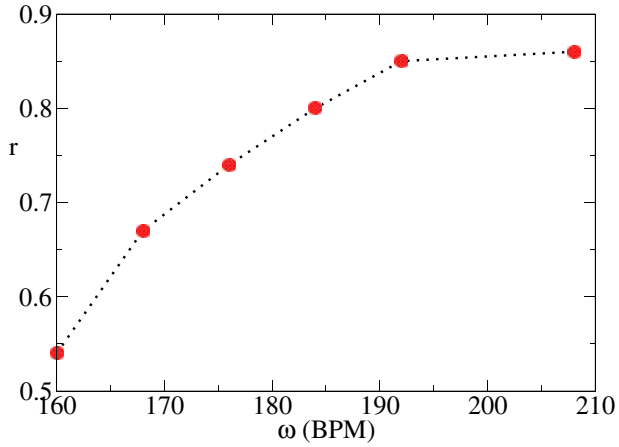

Fig. 3. Experimental results for the Kuramoto order parameter as a function of the nominal frequencies of the metronomes. Experiments performed with seven metronomes and for each frequency the results are averaged on 10 independent measurements.

Here κ_c is the critical coupling value, which depends on the standard deviation of the coupled oscillators natural frequencies. Due to the fact we deal with finite systems, instead of a sharp transition a broader transition region should be observed. Our experiments will focus on detecting this smooth change in the order parameter, as the coupling strength between the metronomes is varied.

In the **first set of experiments** the coupling strength between the metronomes was varied by changing the metronomes nominal ticking frequencies. By increasing the metronomes ticking frequencies we expect to increase the coupling between them, since in unit time more momentum is given to the rotating disk, which couples the metronomes pendulum. We fixed all the metronomes' frequencies on the same marked value and placed them symmetrically on the perimeter of the rotating platform. Naturally, this does not mean that their frequencies were exactly the same, since no two real macroscopic physical systems can be exactly identical. The standard deviations of the natural frequencies of the non-coupled, independent oscillators is indicated in Table 1. For each nominal frequency value we made 10 measurements, collecting data for 10 minutes. The averaged value of the computed Kuramoto order parameter is plotted on Fig. 3.

The experimental results suggest that by increasing the metronomes' natural frequencies, the degree of the obtained synchronization level increases. This is in agreement with our expectations and the results of the Kuramoto model. Since there is no clear trend in the standard deviation of the uncoupled metronomes natural frequencies as a function of ω, the observed effect is not due to a decreasing trend of the metronomes' standard deviation. It is interesting to note however, that if one inspects only visually or auditory the system, he/she would observe no synchronization for frequencies already below 184 BPM. This means that we are not suited to detect partial synchronization with an order parameter below $r = 0.75$.

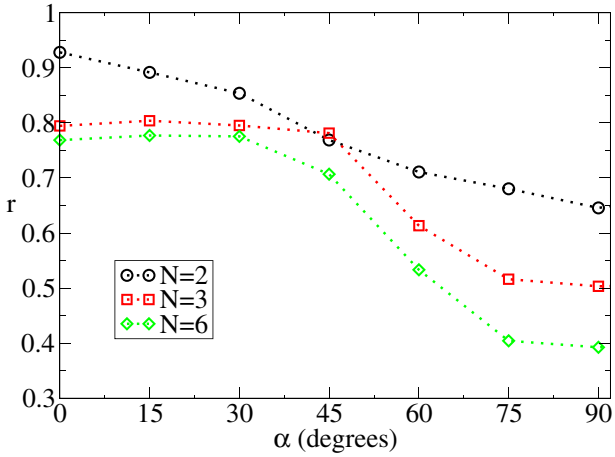

Fig. 4. Experimental results for the Kuramoto order parameter for different rotational angles of the metronomes on the disk. Different symbols correspond to different metronome number on the disk, as indicated in the legend.

In the **second set of experiments** we fixed the nominal frequency of the metronomes to 192 BPM and controlled the coupling between the metronomes by rotating the metronomes orientation on the disk. By doing this, one will change the orientation of the swinging plane of the physical pendulum and will modify the tangential component of the pulses given on the exciting mechanism. One can easily realize, that the coupling will be maximal if the rotation angle is $\alpha = 0$ or $\alpha = 180$ (pulses are tangential), and there will be no coupling for $\alpha = 90$ (tangential component of the pulses is zero). In order to control the rotation angles, α, of the metronomes we mounted a needle on their bottom, perpendicular to the bob's swinging plane. In these experiments we used 2 to 6 metronomes evenly spread on the perimeter of the disk and for each of them we marked with red lines well-defined α angles, ranging from 0° to 90° with a step of 15°. Results for the Kuramoto order parameter as a function of the rotation angle α are plotted on Fig. 4.

The results suggest an order-disorder type phase-transition around $\alpha \approx 50^\circ$. The transition from the partially synchronized state to an unsynchronized one appears as a result of the decreased coupling strength. In agreement with the expected finite-size effects, by increasing the metronomes number on the disk, sharper and sharper transition curves are observable.

In the **third experiment** we varied the metronomes distance relative to the center of the disk. By doing this we change both the total moment of inertia relative to the rotational axes and the torque of the reaction forces of the driving mechanism. Both quantities are decreased as we approach the rotational axes. Decreasing the moment of inertia would lead to an increase in oscillation amplitudes of the disk, thus better coupling between the metronomes. Contrarily to this the decrease of the torque would directly lower the coupling between the metronomes. Experiments show however that this later effect is stronger, and by approaching the metronomes to the axes of the disk, the order parameter decreases. Experimental results for 4 metronomes are plotted in Fig. 5. Unfortunately by this method one cannot reduce the coupling to zero, since metronomes cannot be placed arbitrarily close to the center of the disk. Also, due to the fact that the above indicated two effects has an opposite trend on the order parameter, we obtain a rather small change in the synchronization level, as it is illustrated in Fig. 5.

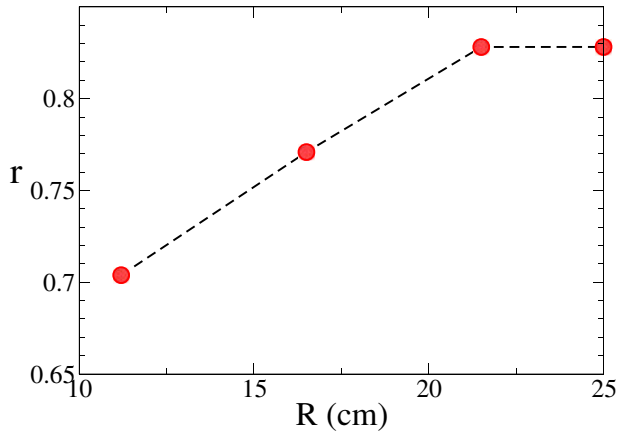

Fig. 5. Experimental results for the Kuramoto order parameter as a function of the metronomes distance R from the center of the disk. Results obtained with 4 metronomes and averaged on 10 independent experiments.

3 Theoretical model

Starting from the approach described in [7], it is possible to consider a realistic model for the coupled metronome system. In this model we represent the metronomes with a rigid box containing a physical pendulum in it. These boxes are placed on the perimeter of the disk, so that the swinging plane of the metronome forms an angle of $90° - \alpha$ with the radial direction on the disk (Fig. 6).

In the Reference frame of the Earth, the Lagrangian for such a system of physical pendulums and rotating disk without damping and driving forces writes as:

$$L = \frac{J}{2}\dot{\phi}^2 + \sum_{i=1}^{N} \frac{m_i}{2}\left\{\left[\frac{d}{dt}(x_i \cos\alpha_i + h_i \sin\theta_i)\right]^2 + \left[\frac{d}{dt}(x_i \sin\alpha_i)\right]^2 + \left[\frac{d}{dt}(h_i \cos\theta_i)\right]^2\right\} + \sum_{i=1}^{N} \frac{J_i\omega_i^2}{2} - \sum_{i=1}^{N} m_i g h_i(1 - \cos\theta_i). \quad (2)$$

The first term is the kinetic energy of the platform, the second one is the total kinetic energy for all pendulum's centre of masses, the third one is the total rotational kinetic energy of the pendulums around their centre of masses, while the last term is the total gravitational potential energy of all pendulum's center of masses. The following notations are used: the index i labels the pendulums, J is the moment of inertia of the platform with the metronomes on it – taken relative to the vertical rotation axis passing the center of the platform ($J = J_0 + N \cdot MR^2$, where J_0 is the moment of inertia of the disk alone and M is the mass of the metronomes boxes and driving mechanism), ϕ is the angular displacement of the platform, m_i is the total mass of the pendulum i ($m_i \approx W_1^{(i)} + W_2^{(i)}$, and we neglect the mass of the pendulum's rod), x_i is the horizontal displacement of the pendulum's suspension point due to the rotation of the platform, α is the orientation of the metronomes swinging plane, h_i is the distance between the pendulum's suspension point and their centre of mass, θ_i is the displacement angle of the i-th pendulum relative to the vertical direction, J_i is the moment of inertia of the pendulum relative to its centre of mass and ω_i is the angular velocity for the rotation of the pendulum relative to its centre of mass.

We assume, that the distance between the centre of mass of the metronome's box and the centre of the disk is R, and this value remains constant, independently

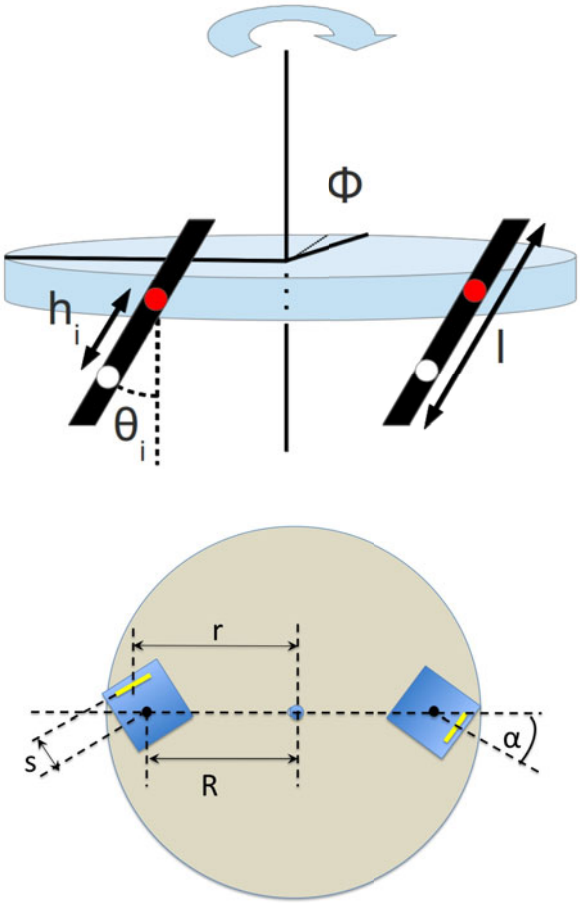

Fig. 6. (Top figure) schematic view and notations for the considered mechanical model. The white dot denotes the centre of mass of the physical pendulums and the grey dot is the suspension axis. (Bottom figure) a view from the top of the system with two metronomes, (boxes represents the metronomes), the black point inside the box is the centre of mass of the metronomes, and the yellow line inside the boxes are the pendulums swinging plane.

of α_i. (Please note, that the centre of mass of the metronome is not in the pendulums swinging plane. The heaviest part of the system is the driving mechanism, and in our simple model we assume that the position of this part remains unchanged when we rotate the metronome with an α angle.) One can immediately realize that $x_i = r_i\phi$, where $r_i = R + s_i \cdot \cos\alpha$ and s_i is the distance between the pendulums swinging plane and the center of mass of the metronome. Also, it is obvious that $\omega_i = \dot{\theta}_i$. We assume, that the mass of all the weights suspended on the bobs are the same ($W_1^{(i)} = w_1$, $W_2^{(i)} = w_2$, and consequently $m_i = m$), and consider also $\alpha_i = \alpha$. Neglecting the $m_i g h_i$ constant terms, one obtains:

$$L' = \Big(\frac{J + NmR^2}{2}\Big)\dot{\phi}^2 + \sum_i \Big(\frac{mh_i^2}{2} + \frac{J_i}{2}\Big)\dot{\theta}_i^2 + mr\dot{\phi}\cos\alpha \sum_i h_i\dot{\theta}_i\cos\theta_i$$
$$+mg\sum_i h_i\cos\theta_i. \tag{3}$$

The Euler-Lagrange equations of motion yields:

$$(J + NmR^2)\ddot{\phi} + mr\cos(\alpha)\sum_i h_i[\ddot{\theta}_i\cos\theta_i - \dot{\theta}_i^2\sin\theta_i] = 0 \tag{4}$$

$$[mh_i^2 + J_i]\ddot{\theta}_i + mr\cos(\alpha)\ddot{\phi}h_i\cos\theta_i + mgh_i\sin\theta_i = 0. \tag{5}$$

These equations are for an ideal conservative system, where frictions and excitations are absent. Friction and excitation terms are added thus separately, and finally one obtains:

$$\begin{aligned}(J + NmR^2)\ddot{\phi} + mr\cos(\alpha)\sum_i h_i[\ddot{\theta}_i\cos\theta_i - \dot{\theta}_i^2\sin\theta_i] + c_\phi\dot{\phi} + \cos(\alpha)\sum_i \mathbb{M}'_i = 0\\ (mh_i^2 + J_i)\ddot{\theta}_i + mr\cos(\alpha)\ddot{\phi}h_i\cos\theta_i + mgh_i\sin\theta_i + c_\theta\dot{\theta}_i = \mathbb{M}_i.\end{aligned} \tag{6}$$

c_ϕ and c_θ are friction coefficients for the rotation of the platform and pendulums, respectively. $\mathbb{M}_i$ and $\mathbb{M}'_i$ are instantaneous excitation terms with the form

$$\begin{aligned}\mathbb{M}_i &= M\delta(\theta_i)\dot{\theta}_i,\\ \mathbb{M}'_i &= \mathbb{M}_i \cdot r \cdot K\end{aligned} \tag{7}$$

where δ denotes the Dirac function and M is a fixed parameter characterizing the driving mechanism of the metronomes and K is a constant. The value of $\mathbb{M}'_i$ was obtained by taking into account the fact that the reaction force produces a torque which is proportional with r. In order not to introduce an extra constant, in the case when the metronomes are placed on the perimeter of the disk, we use the simplified assumption: $\mathbb{M}_i = \mathbb{M}'_i$. In case the metronomes are not at the perimeter of the disk we use: $\mathbb{M}'_i = \mathbb{M}_i \cdot r/R_0$, where R_0 is the radius of the disk. The choice of the form for $\mathbb{M}_i$ in Eq. (7) means that excitations are given only when the metronomes' bob passes the $\theta = 0$ position. The term $\dot{\theta}$ is needed in order to ensure a constant momentum input, independently of the metronomes' amplitude. It also insures that the excitation is given in the good direction (direction of the motion). This driving will be implemented in the numerical solution as

$$\mathbb{M}_i = \begin{cases} M/dt & \text{if } \theta_i(t-dt) < 0 \text{ and } \theta_i(t) > 0\\ -M/dt & \text{if } \theta_i(t-dt) > 0 \text{ and } \theta_i(t) < 0\\ 0 & \text{in any other case}\end{cases}$$

where dt is the time-step in the numerical integration of the equations of motion. It is immediate to realize that this driving leads to the same total momentum transfer M, as the one defined by Eq. (7).

The coupled system of Eq. (6) can be written in a more suitable form for numerical integration:

$$\ddot{\phi} = \frac{mr\cos(\alpha)\sum_i h_i\dot{\theta}_i^2\sin\theta_i - c_\phi\dot{\phi} - A + B + C - D}{F}, \tag{8}$$

$$\ddot{\theta}_i = \frac{\mathbb{M}_i - mr\cos(\alpha)\ddot{\phi}h_i\cos\theta_i - mgh_i\sin\theta_i - c_\theta\dot{\theta}_i}{mh_i^2 + J_i} \tag{9}$$

where

$$A = \cos(\alpha) \sum_i \mathbb{M}'_i,$$

$$B = m^2 gr \cos(\alpha) \sum_i \frac{h_i^2 \sin\theta_i \cos\theta_i}{mh_i^2 + J_i},$$

$$C = mrc_\theta \cos(\alpha) \sum_i \frac{h_i \dot{\theta}_i \cos\theta_i}{mh_i^2 + J_i},$$

$$D = mr \cos(\alpha) \sum_i \frac{h_i \mathbb{M}_i \cos\theta_i}{mh_i^2 + J_i},$$

$$F = \left[J + NmR^2 - m^2 r^2 \cos^2(\alpha) \sum_i \frac{h_i^2 \cos^2\theta_i}{mh_i^2 + J_i} \right].$$

Taking into account that the metronomes' bob have the shape sketched in Fig. 2 and the L_1 distances are fixed, the h_i and J_i terms of the physical pendulums in our model will be calculated as:

$$h_i = \frac{1}{w_1 + w_2}(w_1 L_1 - w_2 L_2^{(i)}) \tag{10}$$

$$J_i = w_1 L_1^2 + w_2 (L_2^{(i)})^2. \tag{11}$$

Equations (8), (9) are numerically integrated using a velocity Verlet-type algorithm [14]. It was shown that a time-step of $dt = 0.01$s is sufficient to get a good convergence. In order to characterize the synchronization level in the system, we used the same Kuramoto order parameter, r, as in the experiments.

The **parameters of the model** were chosen in agreement with the characteristic values of our experimental device: $w_1 = 0.025\,\mathrm{kg}$, $w_2 = 0.0069\,\mathrm{kg}$, $L_1 = 0.0358\,\mathrm{m}$, $L_2 = 0.029\,\mathrm{m}$, $R_0 = 0.27\,\mathrm{m}$, $s = 4\,\mathrm{cm}$ and $J \in \{0.0729, 0.10935, 0.2187\}\,\mathrm{kg\,m^2}$ depending on the number of metronomes placed on the platform. The damping and excitation coefficients were estimated from simple experiments. For the estimation of the c_θ value, a single metronome was considered on a rigid support. Switching off the excitation mechanism, a quasi-harmonic damped oscillation of the metronome took place. The exponential decay of the amplitude as a function of time uniquely defines the damping coefficient, hence a simple fit of the amplitude as a function of time allowed the determination of c_θ. Switching the exciting mechanism on, leads to a steady-state oscillation regime with a constant amplitude. Since c_θ has already been measured, this amplitude is now uniquely defined by the excitation coefficient M. Solving Eq. (9) for a single metronome without a platform, and tuning it until the same steady-state amplitude is obtained as in the experiments, makes possible the estimation of M. Now that both c_θ and M are known, the following scenario is considered: all the metronomes are placed on the platform and synchronization is reached. In such situation the platform has a constant-amplitude oscillation. The angular amplitude of this oscillation will determine the c_ϕ damping coefficient. Its value is tuned by solving the Eqs. (8) and (9), so that the experimentally observed amplitude of the disk's oscillations are reproduced. By these simple experiments all model parameters are realistically determined. The following parameter values were estimated: $c_\theta = 5 \cdot 10^{-5}\,\mathrm{kg\,m^2/s}$, $c_\phi = 1 \cdot 10^{-5}\,\mathrm{kg\,m^2/s}$ and $M = 6 \cdot 10^{-4}\,\mathrm{Nm/s}$.

One should also take into account the differences in the metronomes natural frequencies, i.e. their non-zero standard deviation, σ. In order to introduce this differences in the simulation, we added a noise in the L_2 terms. This leads to slightly

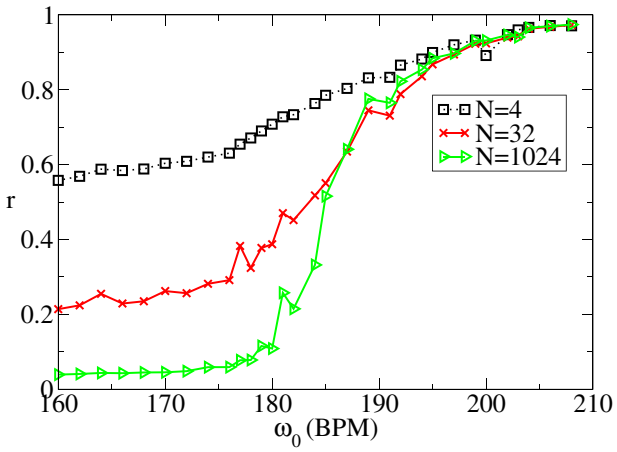

Fig. 7. Synchronization level (Kuramoto order parameter) as a function of the nominal frequency of the metronomes. Simulation results, with realistic model parameters (see Sect. 3) and with various metronome numbers on the disk, as it is specified in the legend.

different h_i values, in agreement with Eq. (10). The magnitude of the noise was chosen in such a manner, that the standard deviation of the metronomes frequencies in the simulation, to be similar with the experimental values.

4 Computer simulation results

Computer simulations for the realistic model has the advantage that it can investigate quickly various situations that are not feasible experimentally. For instance one cannot consider experimentally large number of metronomes (they just do not fit on the disk), or it is tedious to vary the friction coefficients. By simulations we can easily change these parameters, and study the dynamics of this system with a good statistics. Keeping the physical parameters of the metronomes fixed, here we investigate the influence of other relevant parameters, focusing on the order-disorder transition. Our aim is to show that one can observe both synchronized and unsynchronized states by changing the values of these parameters. Sometimes the order-disorder transition is sharp, and sometimes it is rather smooth.

First we reconsider the experimentally investigated case, and vary the metronomes nominal frequencies and the swinging angle of the pendulum relative to the radial direction. We use the $\sigma \approx 10^{-6}$ BPM standard deviation for the metronomes natural frequencies, independently of their number. This number is of the same order of magnitude with the experimentally measured one for all seven metronomes when the nominal frequency was fixed at 192 BPM. All the other parameters are kept as it were given in the preceding section.

As a function of the nominal frequency of the metronomes we get similar order-disorder type transition as in the experiments. Results averaged for 100 independent runs are presented on Fig. 7. By increasing the number of metronomes on the disk the transition becomes sharper, illustrating nicely finite size effects.

Fixing now the metronomes nominal frequencies to the experimentally used 192 BPM value, we studied the influence of the rotation angle α. In order to visualize the increasing fluctuations in the vicinity of the transition point in parallel with the Kuramoto order parameter we have computed now also the standard deviation of the order parameter. The results were averaged again on 100 independent runs

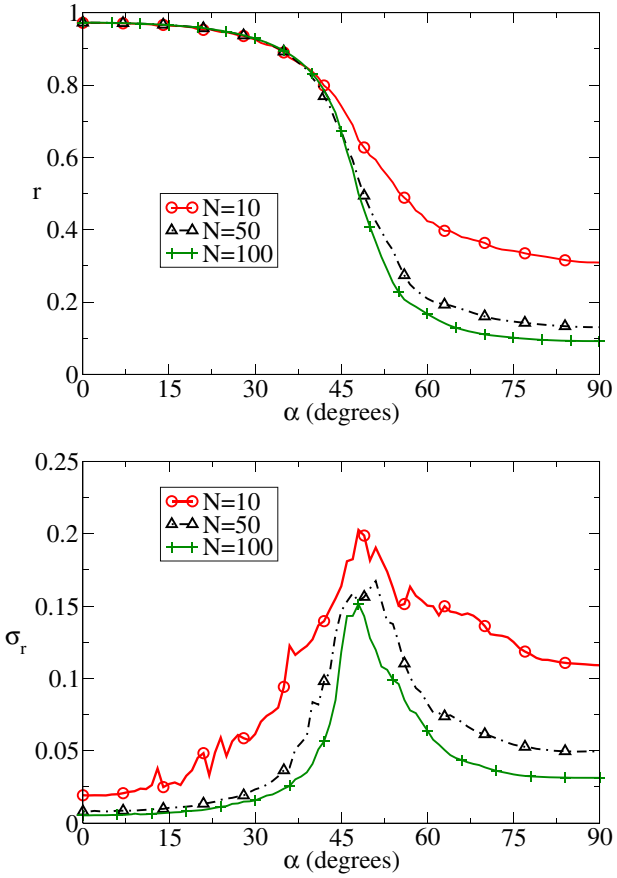

Fig. 8. Simulation results for the Kuramoto order parameter as a function of the α rotation angle of the metronomes (top figure). Simulation results for the standard deviation of the order parameter as a function of α (bottom figure). Results for different metronome number as indicated in the legends. Model parameters were fixed realistically according to Sect. 3.

and are presented here on Fig. 8. The results confirm nicely our expectation, and for larger ensembles the fluctuation curves are sharper and sharper in the vicinity of the phase-transition point.

We have seen in the experiments that another way to control the strength of the coupling between the metronomes is to vary their R distance relative to the rotational axes of the disk. By this we change both the total moment of inertia relative to the rotational axes ($J_{tot} = J + N \cdot mR^2 = J_0 + N \cdot [M + m]R^2$) and the $\mathbb{M}_i'$ torque of the reaction forces. Experiments indicated (see Fig. 5) that by approaching the metronomes to the rotational angle, the synchronization level drops. Unfortunately in the experiments, due to the finite size of the metronomes, we could vary the value of R only in a very restricted interval. In such manner the change in the synchronization order parameter was not impressive. By simulations we can do a better job, and we can study also large ensembles. Results for different metronome numbers are presented on Fig. 9. Similarly with the previous cases a nice order-disorder phase transition is observable. Finite size effects are also nicely visible: increasing the number of metronomes on the disk, we get sharper transition curves.

By increasing the moment of inertia, J_0, of the disk relative to its' rotational axes one can also control the synchronization level. Larger J_0 values would result

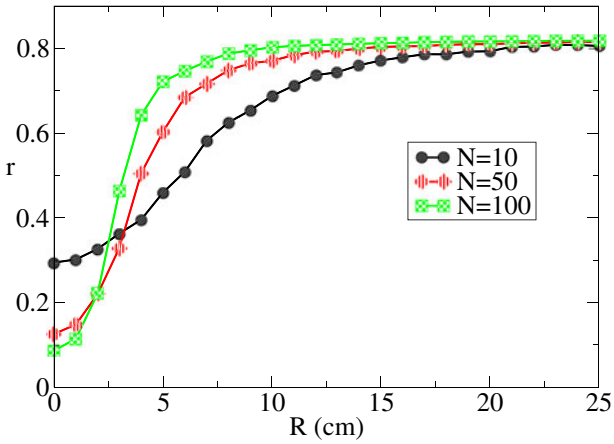

Fig. 9. Simulation results for the synchronization level (Kuramoto order parameter) as a function of the metronomes distance from the rotational axes of the disk. Realistic model parameters were used (see Sect. 3) and various metronome numbers were considered on the disk, as it is specified in the legend.

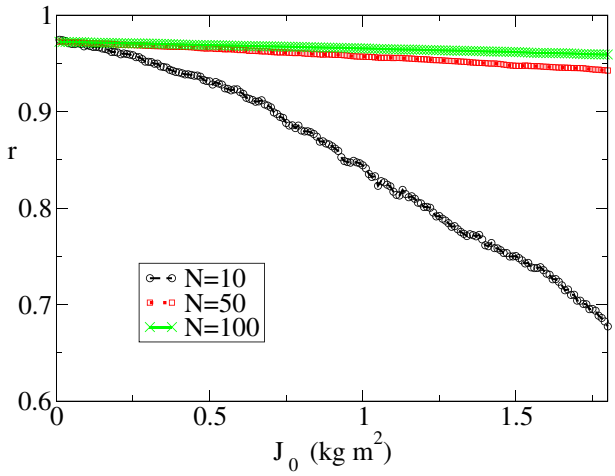

Fig. 10. Simulation results for the Kuramoto order parameter as a function of the J_0 moment of inertia of the disk relative to the rotational axes. Realistic model parameters were used (see Sect. 3) and various metronome numbers were considered on the disk, as it is specified in the legend.

in smaller oscillation periods of the disk, and consecutively a decreased coupling. In such manner one would expect that the synchronization level drops. Due to the fact that in our experiments, the total mass of the metronomes were much larger than the mass of the rotating disk, the decrease in the synchronization level should be observable only for very large variations in J_0. By increasing the metronome number on the disk we expect a decreasing trend in the synchronization level, and a much smoother transition. This is due to the fact that the total inertial moment relative to the vertical rotational axes is given in larger and larger part by the metronomes mass, and less by the disk. Simulation results presented in Fig. 10 confirms these expectations.

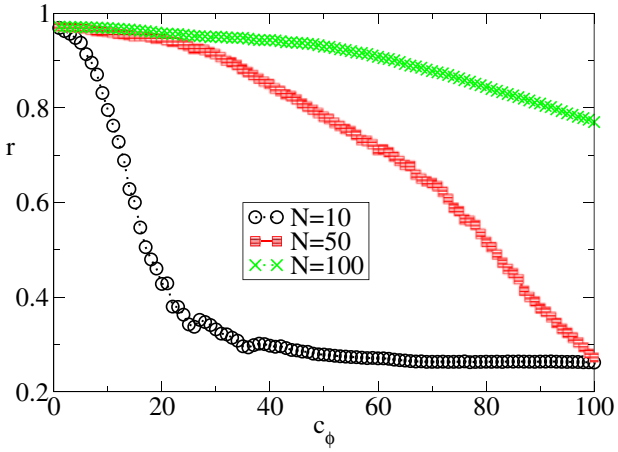

Fig. 11. Simulation results for the Kuramoto order parameter as a function of the c_ϕ friction coefficient of disk. Realistic model parameters were used (see Sect. 3) and various metronome numbers were considered on the disk, as it is specified in the legend.

Finally one can vary the c_ϕ friction coefficient in the rotational axes of the disk. Increasing the value of this friction will lead again to smaller oscillation amplitudes of the disk, and lower synchronization level of the metronomes. By increasing the metronome number on the disk we increase both the total moment of inertia relative to the rotational axes (which has a lowering effect on the oscillation amplitude of the disk) and the intensity of the total excitation pulses (having an increasing effect on the oscillation amplitude). Simulation results (Fig. 11) shows however, that by increasing the metronome number we get better synchronization and consequently a much smoother transition from order to disorder.

5 Conclusions

Metronomes were used for exemplifying the Kuramoto type order-disorder phase transition in non-identical and interacting pendulum systems. It has been shown that this transition can be easily realized experimentally by using a smoothly rotating disk on which the metronomes are placed. Fixing the metronomes on the same nominal beat frequency, their dynamics can be either a synchronized or a non-synchronized one. The order-disorder transition can be realized by varying several physical parameters of the system. Experimentally we used three methods: in the first method the nominal beat frequency was varied, in the second one the metronomes oscillation plane was rotated relative to the radial direction on the disk and in the third method the metronomes were placed at different distances relative to the center of the disk. All experiments suggested that an order-disorder phase transition is observable. A theoretical model with realistic model parameters was elaborated. This model is able to reproduce the experimentally observed trends, and predicted many new methods for visualizing the transition from synchronized to non-synchronized dynamics. The model has the advantage that a large number of metronomes can be used and a good averaging on different initial conditions can be done. As a result of this the curves for the variation of the order parameter as a function of the investigated parameter are smoother and finite size effects are elegantly visualized. Using the model without friction and driving terms has also a pedagogical aim. One would find in such case that the system cannot synchronize, unless we use totally identical units and the dynamics

starts from a completely synchronized initial condition. Damping and driving are thus essential in order to get a stable phase-locking synchronization. The reason for this is that without is damping and driving the system is effectively Hamiltonian, and there no attractors, and as consequence of this no spontaneous ordering will occur. Damping/driving are essential to generate attractors of any sort. Alternatively, in another approach one can argue using the principles of thermodynamics. If one considers the oscillators and the platform a closed system, an emerging order would mean a spontaneous decrease in the total entropy of the system, which would contradict the second law of thermodynamics. Dissipation through friction and driving makes the entropy balance more complicated and would finally increase the total entropy, so the second law of thermodynamics is not violated.

In conclusion we can state that metronomes are an ideal and cheap system for exemplifying order-disorder type phase transitions. Apart of the obvious fascination of getting spontaneous synchronization, such systems are suitable for illustrating finite size effects and increased fluctuations in the neighborhood of the transition point. The present work discussed such experiments.

This research was supported by the European Union and the State of Hungary, co-financed by the European Social Fund in the framework of TÁMOP-4.2.4.A/ 2-11/1-2012-0001 National Excellence Program. We also acknowledge support from the research grant PN-II-ID-PCE-2011-3-0348.

References

1. Y. Kuramoto, I. Nishikawa, J. Statistical Phys. **49**, 569 (1987)
2. C. Huygens, Société Hollandaise des Sciences (1665)
3. M. Bennet, M.F. Schatz, H. Rockwood, K. Wiesenfeld, Proc. Royal Soc. A **458**, 563 (2002)
4. M. Kumon, R. Washizaki, J. Sato, R.K.I. Mizumoto, Z. Iwai, Proc. 15th IFAC World Congr., Barcelona (2002)
5. A.L. Fradkov, B. Andrievsky, Int. J. Non-Linear Mech. **42**, 895 (2007)
6. M. Kapitaniak, K. Czolczynski, P. Perlikowski, A. Stefanski, T Kapitaniak, Phys. Reports **517**, 1 (2012)
7. K. Czolczynski, P. Perlikowski, A. Stefanski, T. Kapitaniak, Physica A **388**, 5013 (2009)
8. K. Czolczynski, P. Perlikowski, A. Stefanski, T. Kapitaniak, Int. J. Bifur. Chaos **21**, 2047 (2011)
9. J. Pantaleone, Amer. J. Phys. **70**, 992 (2002)
10. B. van der Pol, Phil. Mag. **3**, 64 (1927)
11. H. Ulrichs, A. Mann, U. Parlitz, Chaos **19**, 043120 (2009)
12. Sz. Boda, Sz Ujvári, A. Tunyagi, Z. Néda, Eur. J. Phys. **34**, 1451 (2013)
13. Sz. Boda, Z. Néda, B. Tyukodi, A. Tunyagi, The Eur. Phys. J. B **86**, 1 (2013)
14. W.C. Swope, H.C. Andersen, P.H. Berens, K.R. Wilson, J. Chem. Phys. **76**, 637 (1982)